ACS Sustainable Chemistry & Engineering

Research Article

Cite This: ACS Sustainable Chem. Eng. 2020, 8, 267−277

pubs.acs.org/journal/ascecg

Highly Dispersed Single-Phase Ni_2P Nanoparticles on N,P-Codoped Porous Carbon for Efficient Synthesis of *N*-Heterocycles

Tao Song,*[,†] Peng Ren,[†,‡] Zhiming Ma,[†,‡] Jianliang Xiao,[§] and Yong Yang*[,†]

[†]Qingdao Institute of Bioenergy and Bioprocess Technology, Chinese Academy of Sciences, No. 189 Songling Road, Laoshan District, Qingdao 266101, China

[‡]University of Chinese Academy of Sciences, Beijing 100049, China

[§]Department of Chemistry, University of Liverpool, Liverpool L69 7ZD, U.K.

Supporting Information

ABSTRACT: Aerobic oxidative cross-dehydrogenative coupling represents one of the most straightforward and atom-economic methods for construction of C−C and C−X (X = N, O, S, or P) bonds, especially when environmentally friendly air is used as the oxidant. Herein, we report the development of an inexpensive, stable, and highly dispersed ultrafine Ni_2P nanoparticles with narrow size distribution supported on N,P-codoped biomass-derived porous carbon. The as-prepared catalyst is highly active and stable for the synthesis of pharmaceutically important *N*-heterocycles, including quinazolines, quinazolinones, and imidazoles, through oxidative cross-dehydrogenative coupling of a wide range of alcohols with diamines or 2-aminobenzamides using atmospheric air as the sole oxidant under mild reaction conditions. This work provides a new method to access *N*-heterocycles, which is operationally simple, widely applicable to various alcohols and diamines (or 2-aminobenzamides), and capable for gram-scale synthesis, highlighting its practical potential. Mechanistic studies reveal that the coupling proceeds in a cascade manner, with atmospheric air as a hydrogen acceptor that significantly boosts the overall reaction efficiency.

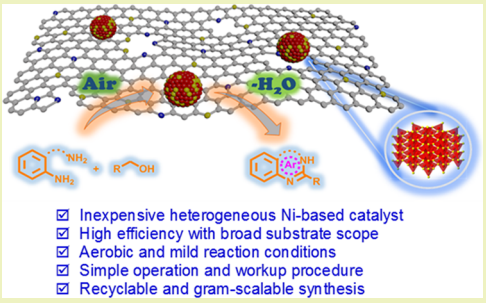

KEYWORDS: *Ni_2P nanoparticles, biomass-derived carbon, cross-dehydrogenation coupling, aerobic oxidation, N-heterocycles*

INTRODUCTION

N-heterocycles are key core structures that form the basis of many pharmaceutical, agrochemical, and natural products.[1−5] Among them, quinazolines, quinazolinones, and imidazoles are well known to have a wide spectrum of biological and medicinal properties, such as antibacterial,[6−8] antiviral,[9−11] and anticancer activities.[12−14] Nowadays, as privileged structures, quinazoline, quinaolinone, and imidazole core skeleton are found in many drugs available in the market or are under investigation in clinical trials (Scheme 1).

Given their extreme importance, various synthetic approaches have been developed for the synthesis of quinazolines, quinazolinones, and imidazoles over the past decades. Traditionally, oxidative condensation of diamines (or 2-aminobenzamides) with carbonyl compounds[15−24,36−53,60−65] or metal-catalyzed coupling of multicomponents[20,25−35,54−59,66−71] was frequently employed. However, these methods generally involved large excess of hazardous oxidants and suffered from limitations of substrate generality and availability of starting material, which strongly hamper their extensive application.

Recently, metal-catalyzed cross-dehydrogenative couplings (CDCs), as a powerful synthetic strategy,[72−74] have attracted great attention for the sustainable synthesis of quinazolines, quinazolinones, and imidazoles. It represents the most straightforward and effective method owing to significantly high overall reaction efficiencies and improved atom economy. In this regards, abundantly available and low toxic primary alcohols were used as coupling partners to react with diamines or 2-aminobenzamides to produce their corresponding *N*-heterocycles with evolution of molecular hydrogen or water as sole by-products. As a result, various metal catalysts, including Pt,[75,76] Pd,[77−79] Ir,[80−82] Ru,[83−85] Au,[86−88] Co,[89] Cu,[90,91] Ni,[92−94] and Mn,[95] have been employed for CDCs. However, the reactions were usually carried out in homogeneous solution and generally required the assistance of sophisticated and expensive ligands to achieve satisfactory reactivity thus far. As such, product−catalyst separation remains a big challenge because the homogeneous catalysts are difficult to separate from the product mixture for recycles, which is a particularly significant drawback for their application in the pharmaceutical industry. Meanwhile, metal-catalyzed (e.g., Fe,[96,97] Mn,[98] Cu,[99−101] and Co[102,103]) oxidative CDCs have also been developed for construction of *N*-heterocycles, although stoichiometric or excess amounts of hazardous oxidants, such as TBHP, H_2O_2, IBX, DIB, or I_2, are indispensable. Molecular

Received: September 6, 2019
Revised: November 13, 2019
Published: December 3, 2019

DOI: 10.1021/acssuschemeng.9b05298
ACS Sustainable Chem. Eng. 2020, 8, 267−277

Scheme 1. Selected Examples of *N*-Heterocyclic Moiety-Based Drugs

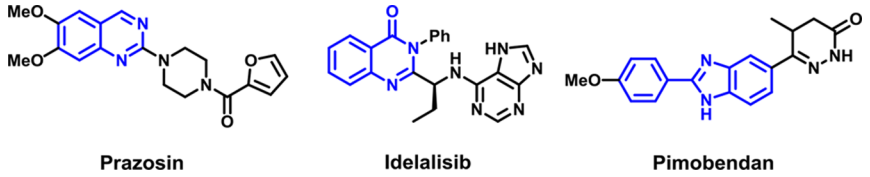

Scheme 2. Strategies for the Synthesis of Quinazolines, Quinazolinones, and Iminazoles Using Alcohols as Starting Materials

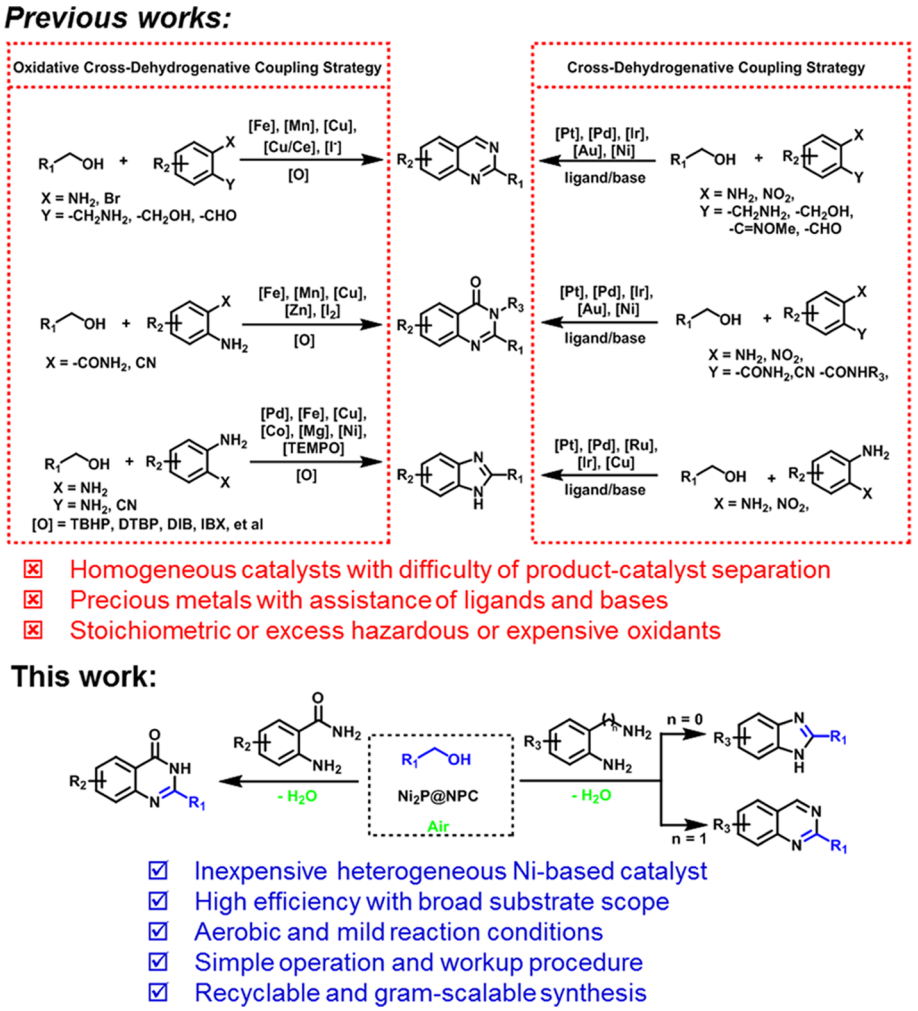

oxygen as the most desired oxidants have been widely used in modern organic synthesis;[104−106] however, sporadic examples using molecular oxygen as the oxidant have also been reported for the above conversion.[97,99,101,103,107−109] Nonetheless, despite the significance of these reports, it is highly desirable to develop a facile, efficient approach to synthesize *N*-heterocycles using an inexpensive heterogeneous catalyst, with excellent activity, broad substrate scope, and high atom economy, in an operationally simple and environmentally friendly manner.

Herein, we developed a stable inexpensive heterogeneous metal catalyst (denoted as Ni_2P@NPC-800) in which ultrafine Ni_2P nanoparticles (NPs) with narrow size distribution were homogeneously dispersed on N,P-codoped biomass-derived porous carbon. The resultant catalyst Ni_2P@NPC-800 shows excellent catalytic activities for synthesis of quinazolines, quinazolinones, and imidazoles via oxidative cross-dehydrogenative coupling of alcohols and diamines or 2-aminobenzamides using air as the sole oxidant under milder reaction conditions (Scheme 2). To the best of our knowledge, this is the first operationally simple, convenient, yet efficient catalytic process for *N*-heterocycles in the presence of a robust heterogeneous catalyst and atmospheric air as an oxidant. The high catalytic activity, good functional group tolerance, broad substrate scopes, and strong stability, accompanied by operationally easy-handling and mild reaction conditions, highlight this protocol to be practical for the synthesis of pharmaceutically important *N*-heterocycles.

RESULTS AND DISCUSSION

Ultrafine and highly dispersed Ni_2P NPs on biomass-derived porous carbon was prepared in a sequential hydrothermal and pyrolysis process according to our previous reports.[110−114] The biochar obtained from hydrothermal treatment of bamboo

DOI: 10.1021/acssuschemeng.9b05298
ACS Sustainable Chem. Eng. 2020, 8, 267−277

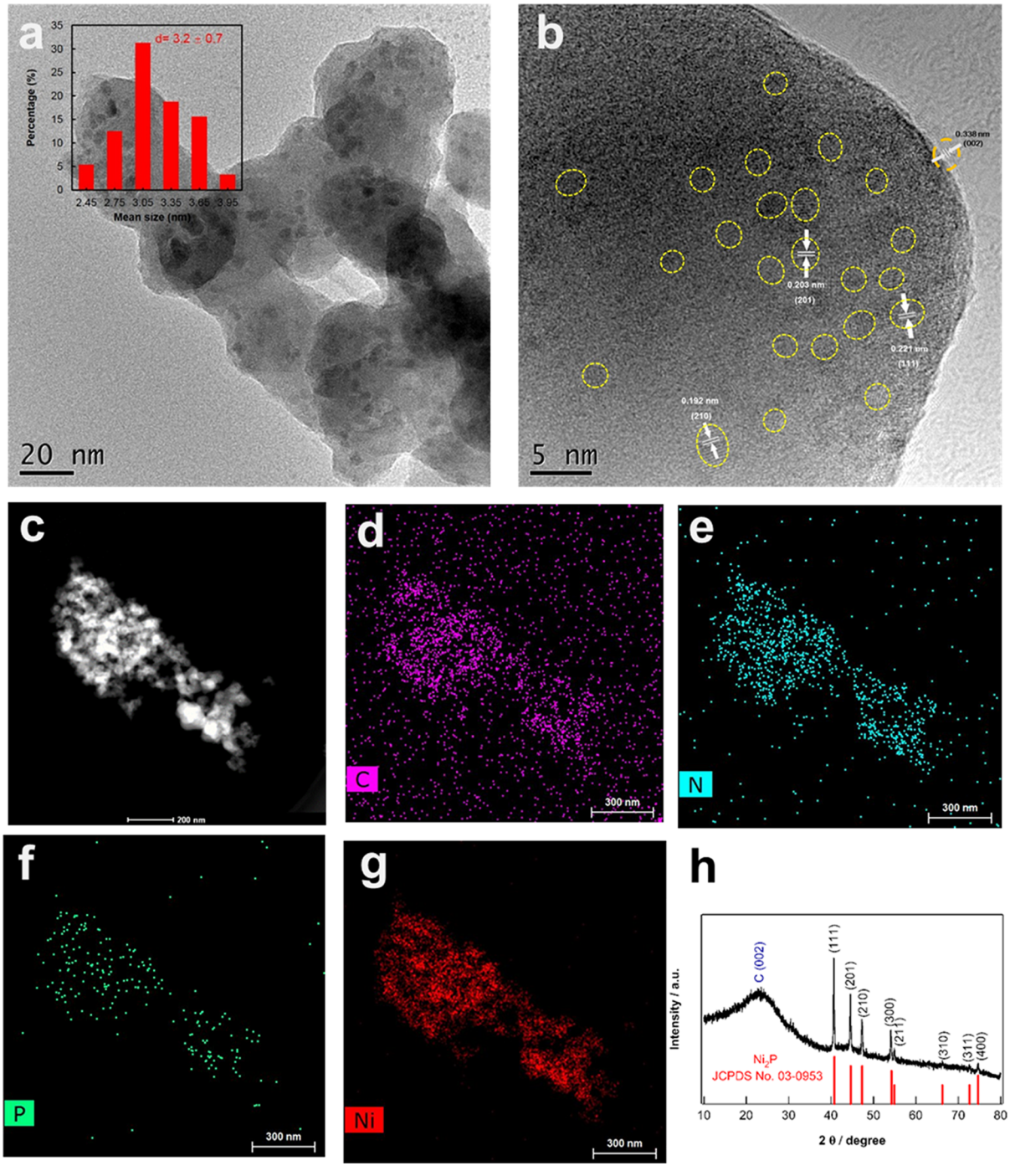

Figure 1. (a) TEM, (b) HR-TEM, and (c) HAADF STEM images of Ni_2P@NPC-800. (d–g) EDX mappings of C, N, P, and Ni of Ni_2P@NPC-800. (h) Powder XRD pattern of Ni_2P@NPC-800.

shoots was homogeneously mixed with $Ni(OAc)_2$ and phytic acid (PA), as Ni and P sources, respectively, in aqueous solution at 60 °C for 2 h. After evaporation of the water, the solid powder was pyrolyzed under a constant nitrogen flow at 800 °C for 2 h. (See details in the Supporting Information). The as-prepared catalyst was denoted as Ni_2P@NPC-800. For comparison, Ni_2P@NPC-700 and 900 pyrolyzed at 700 and 900 °C were also prepared with the same preparation procedure. The Ni content in the catalysts was determined to be 3.0–4.9 wt % by the coupled plasma optical emission spectrometry (ICP-OES) (Table S1).

The typical transmission electron microscopy (TEM) images (Figure 1a) of Ni_2P@NPC-800 disclose that the ultrafine Ni_2P NPs are uniformly dispersed with narrow size distribution (3.2 ± 0.7 nm) on the graphitic carbon material. The high-resolution TEM image (Figure 1b) clearly shows the lattice fringe spacings of 0.192, 0.203, 0.223, and 0.338 nm corresponding to the (210), (201), and (111) planes of Ni_2P and (002) plane of graphitic carbon, respectively. High-angle annular dark-field scanning transmission electron microscopy (HAADF-STEM) (Figure 1c) with energy-dispersive X-ray (EDX) maps (Figure 1d–g) clearly shows the homogeneous distribution of Ni, P, N, O, and C through the entire carbon

DOI: 10.1021/acssuschemeng.9b05298
ACS Sustainable Chem. Eng. 2020, 8, 267–277

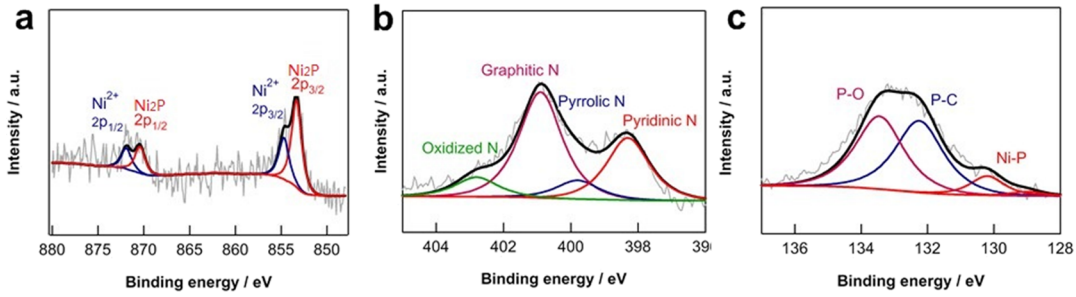

Figure 2. High-resolution XPS spectra of (a) Ni 2p, (b) N 1s, and (c) P 2p for Ni_2P@NPC-800.

Table 1. Optimization of Reaction Conditions[a]

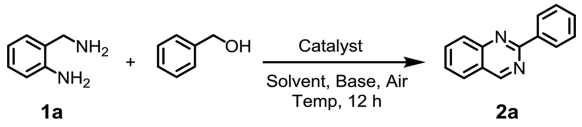

entry	catalyst	solvent	base	conv.(%)[b]	selec.(%)[b]
1[c]	Ni_2P@NPC-800	toluene	*t*BuOK (20 mol %)	12	>99
2	Ni_2P@NPC-800	toluene	*t*BuOK (20 mol %)	94	>99
3	Ni_2P@NPC-800	toluene		5	>99
4	Ni_2P@NPC-800	toluene	*t*BuOK (5 mol %)	27	>99
5	Ni_2P@NPC-800	toluene	*t*BuOK (10 mol %)	61	>99
6[d]	Ni_2P@NPC-800	toluene	*t*BuOK (20 mol %)	77	>99
7	Ni_2P@NPC-800	toluene	EtONa (20 mol %)	37	>99
8	Ni_2P@NPC-800	toluene	MeONa (20 mol %)	31	>99
9	Ni_2P@NPC-800	toluene	NaOH (20 mol %)	13	
10	Ni_2P@NPC-800	toluene	Na_2CO_3 (20 mol %)	0	>99
11	Ni_2P@NPC-800	CH_3CN	*t*BuOK (20 mol %)	9	>99
12	Ni_2P@NPC-800	THF	*t*BuOK (20 mol %)	0	>99
13	Ni_2P@NPC-800	acetone	*t*BuOK (20 mol %)	0	>99
14	Ni_2P@NPC-800	*t*BuOH	*t*BuOK (20 mol %)	11	>99
15	Ni_2P@NPC-700	toluene	*t*BuOK (20 mol %)	47	>99
16	Ni_2P@NPC-900	toluene	*t*BuOK (20 mol %)	91	>99
17	Ni@NC-800	toluene	*t*BuOK (20 mol %)	39	>99
18		toluene	*t*BuOK (20 mol %)	7	>99
19	NC-800	toluene	*t*BuOK (20 mol %)	6	>99
20	NPC-800	toluene	*t*BuOK (20 mol %)	4	>99
21		toluene		0	>99

[a]Reaction conditions: benzyl alcohol (0.2 mmol), 2-(aminomethyl)aniline (0.22 mmol), catalyst (7.5 mol % of Ni), *t*BuOK (4.48 mg, 20 mol %), toluene (2 mL), under atmospheric air, 120 °C, 12 h. [b]Determined by NMR. [c]Under atmospheric argon. [d]At 100 °C.

framework. Powder X-ray diffraction (PXRD) pattern of the catalyst Ni_2P@NPC-800 (Figure 1h) discloses the formation of Ni_2P phase with distinct and sharp diffraction peaks at 40.8, 44.6, 47.3, 54.2, 54.9, 66.2, 72.7, and 74.7°, corresponding to (111), (201), (210), (300), (211), (310), (311), and (400) planes of Ni_2P (JCPDS No. 03-0953), respectively, in good consistency with the HR-TEM observation. Besides, a broad diffraction peak at around 25°, assignable to the (002) plane of graphitic carbon, was also observed, indicating the formation of carbon with a relatively higher degree of graphitization, which was further confirmed by Raman spectroscopy (Figure S1). N_2 adsorption/desorption measurements demonstrate that the catalyst Ni_2P@NPC-800 prepared in this strategy possesses hierarchically micro, meso, and macropores with high specific surface area and large pore volume, as shown in Figure S2 and Table S1.

X-ray photoelectron spectroscopy (XPS) measurement was employed to unveil the surface compositions and chemical state of the Ni_2P@NPC-800.The spectrum of Ni 2p region in Figure 2a shows a doublet containing a lower energy (Ni $2p_{3/2}$) band and a higher energy (Ni $2p_{1/2}$) band. Of them, the peaks at 853.3 and 870.4 eV correspond to the Ni $2p_{3/2}$ and Ni $2p_{1/2}$ of Ni_2P, respectively, with the remaining two peaks at 856.7 and 873.9 eV corresponding to Ni $2p_{3/2}$ and Ni $2p_{1/2}$ of Ni^{2+}.[115−118] The high-resolution N 1s spectrum (Figure 2b) indicates the presence of four forms of nitrogen, namely, pyridinic N (398.2 eV), pyrrolic N (399.6 eV), graphitic N (401.2 eV), and oxidized N (402.8 eV), which come from the decomposition of N-containing compounds in bamboo shoots.[110−114] The high-resolution P 2p spectrum (Figure 2c) reveals the existence of P $2p_{3/2}$ (129.5 eV) and P $2p_{1/2}$ (130.1 eV) of the P−Ni bond, as well as the P−C bond (132.4 eV) and P−O bond (133.4 eV). The observation of the P−C bond indicates that P atoms were incorporated into the carbon framework.[115−118]

With the as-prepared catalyst Ni_2P@NPC-800 in hand, we initiated our investigation by choosing synthesis of 2-phenylquinazoline (**2a**) from coupling of benzyl alcohol with

DOI: 10.1021/acssuschemeng.9b05298
ACS Sustainable Chem. Eng. 2020, 8, 267−277

Table 2. Substrate Scopes for Synthesis of Quinazolines and Imidazoles[a,b]

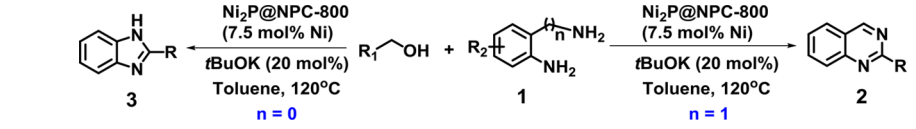

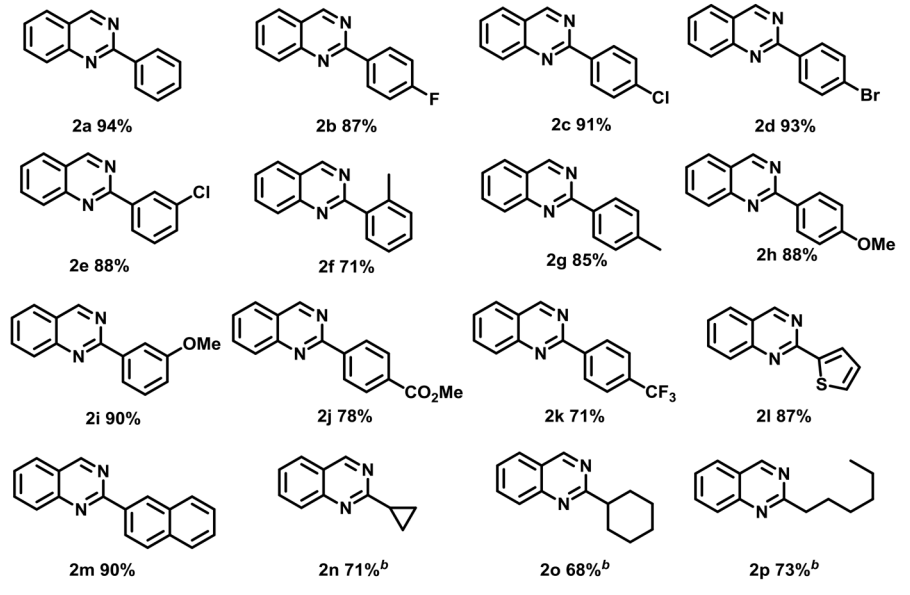

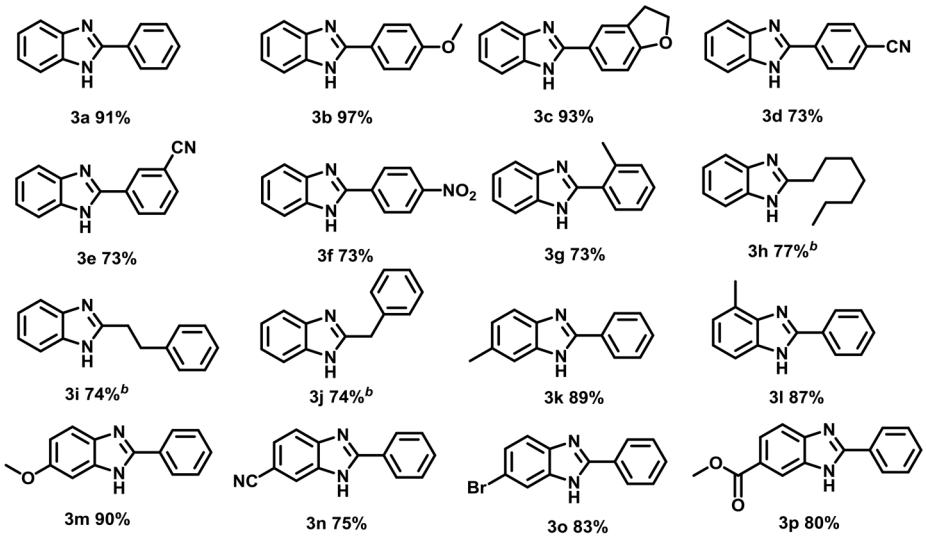

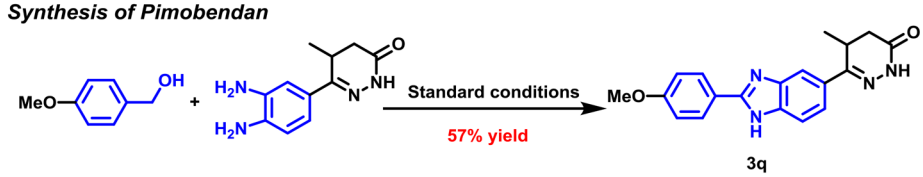

[a]Reaction conditions: alcohol (0.2 mmol), amines (0.22 mmol), Ni_2P@NPC-800 (20 mg, 7.5 mol % of Ni), *t*BuOK (4.48 mg, 20 mol %), toluene (2 mL), under atmospheric air, 120 °C, 12 h. [b]140 °C for 12 h. Yields of isolated product are reported.

2-(aminomethyl)aniline (**1a**) as a benchmark reaction. The reaction was first performed in the presence of Ni_2P@NPC-800 (7.5 mol % of Ni) and *t*BuOK (20 mol %) in toluene at 120 °C under atmospheric argon. In this case, only 12% conversion of benzyl alcohol was observed with excellent selectivity to the desired 2-phenylquinazoline **2a** after 12 h (Table 1, entry 1). Surprisingly, when the reaction was carried out under atmospheric air under otherwise identical conditions, 94% NMR yield of **2a** was achieved (Table 1, entry 2), indicating the key effect of air as an oxidant for boosting the reaction efficiency. Based on this significant finding, a set of parameters, including reaction temperature and types of bases

DOI: 10.1021/acssuschemeng.9b05298
ACS Sustainable Chem. Eng. 2020, 8, 267−277

Table 3. Substrate Scope for Synthesis of Quinazolinones[a,b]

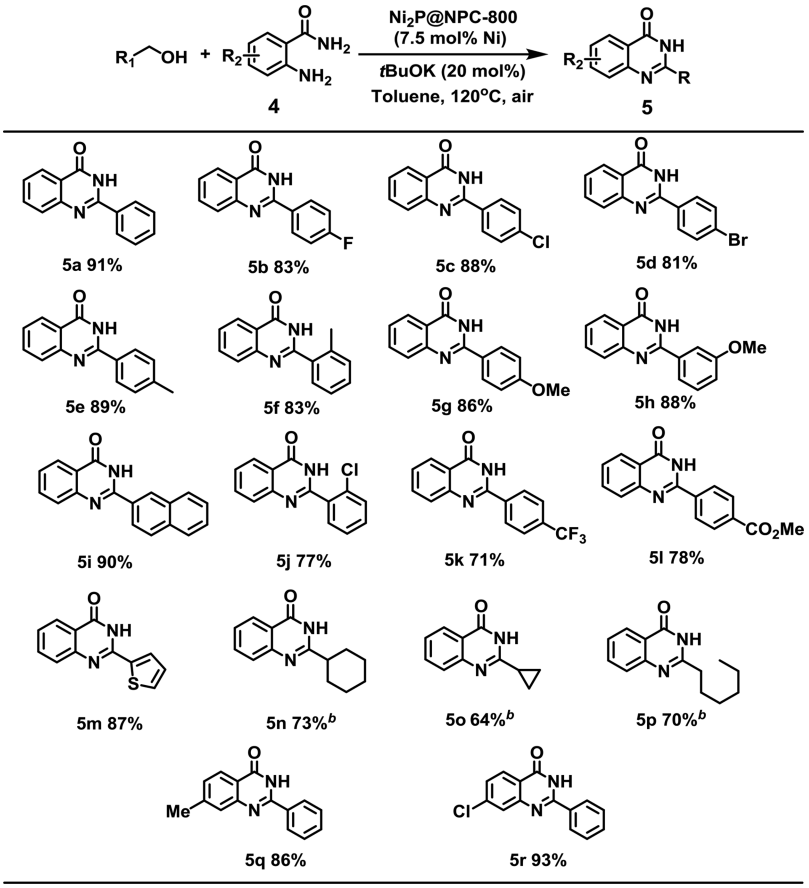

[a]Reaction conditions: alcohol (0.2 mmol), 2-aminobenzamide (0.22 mmol), Ni_2P@NPC-800 (20 mg, 7.5 mol % of Ni), *t*BuOK (4.48 mg, 20 mol %), toluene (2 mL), under atmospheric air, 120 °C, 12 h. [b]140 °C for 12 h. Yields of isolated product are reported.

and solvents, were subsequently screened. A decrease in the amount of *t*BuOK or reaction temperature resulted in a significantly lower reactivity (Table 1, entries 3−6). Other bases such as NaOMe, NaOEt, NaOH, and Na_2CO_3 all gave poor reactivity or no reactivity (Table 1, entries 7−10). Among the solvents investigated, toluene was found to be the best choice (Table 1, entries 11−14). Control experiments, either in the absence of Ni_2P@NPC or base or in the presence of NPC-800 without Ni loading as a catalyst, all gave negligible reactivity (Table 1, entries 3, 18−20). No reaction took place at all for the blank reaction (Table 1, entry 21). These observations clearly indicate the critical role of the base and catalyst for the success of the reaction.

For comparison, the catalyst Ni_2P@NPC-700 showed a relatively lower activity, while a comparable reactivity was observed for the catalyst Ni_2P@NPC-900 (Table 1, entries 15 and 16), compared with that of Ni_2P@NPC-800 under otherwise identical conditions. PXRD pattern and XPS measurement disclose no formation of Ni_2P NPs in the catalyst Ni_2P@NPC-700, while the catalysts Ni_2P@NPC-800 and Ni_2P@NPC-900 have very similar structural properties (Figure S3). Besides, the catalyst Ni@NC-800 with the presence of metallic Ni phases, which was prepared in the same procedure but without addition of PA, also demonstrated a considerably lower activity (Table 1, entry 17). The introduction of appropriate amount of PA is also found to be greatly important for achieving high catalytic efficiency due to the formation of different Ni phases, as shown in Table S2 and Figure S4. Such observations indicate that ultrafine and highly dispersed Ni_2P NPs are primarily responsible for the high catalytic activity.

After identifying the optimized reaction conditions, we next explored the generality of this protocol for the synthesis of *N*-heterocyclic compounds. First, 2-(aminomethyl)aniline (**1a**) was coupled with a set of aromatic and aliphatic alcohols to afford quinazolines. As shown in Table 2, various alcohols could be efficiently coupled, affording their corresponding quinazolines in good to high yields. Benzyl alcohols bearing either electron-donating (−Me and −OMe) or electron-withdrawing groups ($-O_2CMe$ and $-CF_3$) were smoothly transformed into their respective quinazoline, and a relatively higher yield was achieved for the benzyl alcohol with an electron-donating group (**1f−i**) than with an electron-withdrawing one (**1j** and **1k**), while Me substitution on the ortho-position of phenyl ring gave slightly lower yields compared with that substituted on the para position, indicating the steric effect on the reaction efficiency. Halogen-substituted benzyl alcohols (**1b−e**) were well tolerated. Moreover, thiophen-2-ylmethanol (**1l**) and naphthalen-2-ylmethanol (**1m**) were also suitable for the construction of quinazolines in 87 and 90% yields, respectively. More importantly, primary and secondary aliphatic alcohols, which are challenging in previously reported methods,[75,78,92,93,100] such as cyclopropylmethanol (**1n**), cyclohexylmethanol (**1o**), and heptanol (**1p**), were found to be compatible with the present conditions to furnish their desired quinazolines in good yields at slightly elevated reaction

DOI: 10.1021/acssuschemeng.9b05298
ACS Sustainable Chem. Eng. 2020, 8, 267−277

temperatures. This represents a significant advancement for the synthesis of quinazolines.

Subsequently, *o*-phenylenediamine was subjected to the optimal reaction conditions to couple with a variety of alcohols for the synthesis of benzimidazoles (**3a**). We were pleased to find that various benzimidazoles were smoothly obtained in good to excellent yields. Electron-donating group-substituted benzyl alcohols (**3b** and **3c**) showed relatively higher catalytic activity compared with those electron-withdrawing group-substituted ones (**3d**−**f**). Aliphatic alcohols such as heptanol (**3h**), 3-phenylpropan-1-ol (**3i**), and 2-phenylethan-1-ol (**3j**) were also good coupling partners to afford their corresponding benzimidazoles in 74−77% yields. Besides, many valuable functional groups, for example, for example, −Br-, −CN-, −OMe-, and $-CO_2Me$-substituted *o*-phenylenediamines (**3m**−**p**), were also compatible with this protocol conditions. We also applied this heterogeneous catalytic protocol for the synthesis of Pimobendan, which is a novel cardiotonic vasodilator available in many countries for use in canine heart failure.[119] Pimobendan (**3q**) was obtained in 57% yield under optimized conditions, highlighting the practical application of this protocol for the synthesis of bioactive molecules.

Finally, we further extended this protocol to the synthesis of quinazolinones using 2-aminobenzamides as coupling partners, and the results are compiled in Table 3. Aromatic, heterocyclic, and aliphatic alcohols were efficiently coupled with 2-aminobenzamide (**4a**) to deliver their corresponding quinazolinones in 64−91% yields. Similar to the observations in the synthesis of quinazolines and benzimidazoles, benzyl alcohols with electron-donating groups gave relatively higher reactivity than those with electron-withdrawing ones, and the aliphatic alcohols required elevated reaction temperatures to achieve decent yields. Halogen-substituted benzyl alcohols are also compatible with the present conditions to afford their corresponding quinazolinones in high yields. In addition, methyl- and chloro-substituted 2-aminobenzamides (**4q** and **4r**) could serve as coupling partners to yield the desired quinazolinones in 86 and 93% yields, respectively.

Durability/recyclability of a heterogeneous catalyst is critical for practical applications. To test the durability of Ni_2P@NPC-800, the used catalyst was collected, washed, and dried after completion of an oxidative coupling experiment for the synthesis of 2-phenylquinazoline (**2a**). As shown in Figure S6, the catalytic activity and selectivity remained high with negligible changes after five recycles, demonstrating the high durability of this catalyst. Furthermore, ICP analysis of the recycled catalyst gave a very close nickel content to the fresh one (4.49 vs 4.58 wt %). XRD and XPS analyses of the recycled catalyst also confirmed the good reservation in the structure (Figures S7 and S8 in the Supporting Information).

Furthermore, reactions with a 25 times higher amount of the substrate (5 mmol) were performed to demonstrate the applicability of this novel catalyst system for gram-scale synthesis of quinazoline, quinazolinone, and imidazole, as shown in Schemes S1−S3. The yields are in agreement with the 0.2 mmol reactions. Notably, in these cases, the pure desired products could be easily obtained upon filtration of the catalyst followed by washing with water and evaporation of the solvent after the reaction, and column purification workup process is not required, highlighting the highly practical potential for synthesis of *N*-heterocycles using the present method.

To gain insight into the reaction pathway, a set of control experiments were subsequently carried out, adopting the synthesis of 2-phenylquinazoline as a model reaction. Under the standard reaction conditions, benzyl alcohol could be dehydrogenated into benzaldehyde in 98% GC yield (Scheme 3, eq a). However, the reaction became significantly sluggish

Scheme 3. Control Experiments

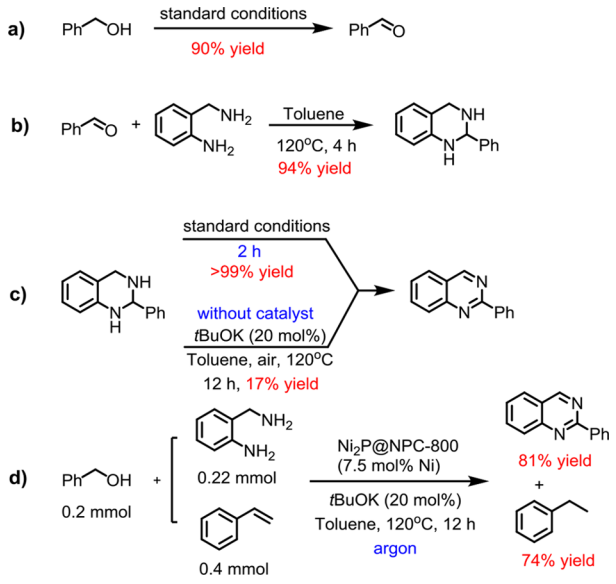

when it was performed using inert atmospheric argon instead of air under otherwise identical conditions, giving only 17% conversion of benzyl alcohol. As indicated in the reaction conditions optimization, 7.8 times higher catalytic activity was accomplished for the reaction in the standard conditions than in the presence of atmospheric argon under otherwise identical conditions (Table 1, entry 1 versus 2). It is well known that alcohol dehydrogenation is a thermodynamically uphill process. The presence of air as a hydrogen acceptor to form H_2O is expected to favorably drive the shift of the reaction equilibrium, thereby altering the thermodynamics of the reaction and boosting the rate of the forward reaction. To confirm the necessity of hydrogen acceptor, the reaction was conducted under atmospheric argon but in the presence of styrene as a hydrogen acceptor instead of air (Scheme 3, eq d). In this case, the reaction proceeded efficiently, affording the desired 2-phenylquinazoline in 81% yield accompanied by the concomitant formation of ethyl benzene in 74% yield. This observation firmly evidences the critical role of a hydrogen acceptor in the entire reaction process. Theoretically, Ni_2P NPs could interact with benzyl alcohol to form [Ni−H] species,[120−122] which could release molecular hydrogen to complete the catalysis cycle. However, the hydrogen evolution process from metal hydride is kinetically difficult due to the need of a sufficient energy to drive the combination of hydrogen. Consequently, the presence of air severing as an ideal hydrogen acceptor could promote the catalytic process.

The generated benzaldehye could readily undergo direct condensation with 2-aminobenzylamine to form 2-phenyl-1,2,3,4-tetrahydroquinazoline in toluene at 120 °C within 4 h without the assistance of a catalyst or base (Scheme 3, eq b). Furthermore, 2-phenyl-1,2,3,4-tetrahydroquinazoline could be quantitatively dehydrogenated into 2-phenylquinazoline under standard conditions within 2 h, while a considerably lower

DOI: 10.1021/acssuschemeng.9b05298
ACS Sustainable Chem. Eng. 2020, 8, 267−277

conversion (ca. 17%) was achieved in the absence of Ni_2P@NPC-800 under otherwise identical conditions, confirming the essential role of the catalyst for the dehydrogenative aromatization process to afford quinazolines (Scheme 3, eq c).

Taking all control experiments into account, we can infer that the synthesis of *N*-heterocycles in this protocol undergoes a cascade reaction process following (i) the oxidative dehydrogenation of alcohol to aldehyde to generate the [Ni−H] species in the presence of base, (ii) condensation between aldehyde and diamine or 2-aminobenzamide to form tetrahydrohydroquinazoline, dihydroquinazolin-4(1H)-one or dihydrobenzoimidazole, and (iii) oxidative dehydrogenative aromatization assisting with the Ni_2P catalyst and base to afford the desired *N*-heterocycles with the release of H_2O to complete the catalytic cycle (Scheme 4). Further kinetic studies show that the dehydrogenative oxidation of alcohol to aldehyde is the rate-limiting step in the whole process (Figure S9).

Scheme 4. Proposed Mechanism of Synthesis of *N*-Heterocycles via Oxidative Cross-Dehydrogenative Coupling of Alcohols and Diamines or 2-Aminobenzamides

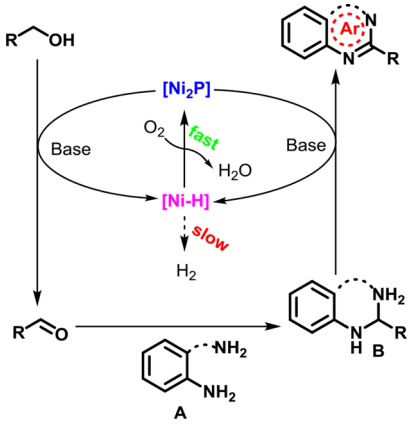

CONCLUSIONS

In conclusion, we have developed an inexpensive, stable, and highly dispersed ultrafine Ni_2P NPs with narrow size distribution supported on N,P-codoped biomass-derived hierarchical porous carbon. The resultant best catalyst Ni_2P@NPC-800 exhibited high catalytic activity for synthesis of *N*-heterocycles, including quinazolines, quinazolinones, and imidazoles through aerobic cross-dehydrogenative coupling of alcohols with diamines or 2-aminobenzamides using atmospheric air as the most environmentally friendly oxidant under milder reaction conditions. A broad spectrum of quinazolines, quinazolinones, and imidazoles could be efficiently synthesized in high yields with good tolerance of multifunctional groups for both coupling partners. Furthermore, the catalyst Ni_2P@NPC-800 is highly stable, allowing for facile recycling and gram-scale transformation. This study provides an operationally simple, practical, and highly efficient synthetic method for the expedient construction of a variety of pharmaceutically important *N*-heterocycles using an inexpensive and stable heterogeneous non-noble metal catalyst with abundant, available, safe air as green oxidant.

ASSOCIATED CONTENT

Supporting Information

The Supporting Information is available free of charge at https://pubs.acs.org/doi/10.1021/acssuschemeng.9b05298.

Raman spectra; N_2 sorption isotherms and pore size distribution; XRD patterns; Ni 2p, P 2p, N 1s, and C 1s XPS spectra for Ni_2P@NPC-700, Ni_2P@NPC-800, and Ni_2P@NPC-900; chemical composition and texture properties of Ni_2P@NPC-700, Ni_2P@NPC-800, and Ni_2P@NPC-900; XRD pattern and Ni 2p XPS spectra of the fresh and used Ni_2P@NPC-800; ^1H and ^{13}C NMR spectra of products (**2a−p**, **3a−q**, and **5a−r**) (PDF)

AUTHOR INFORMATION

Corresponding Authors

*E-mail: songtao@qibebt.ac.cn (T.S.).
*E-mail: yangyong@qibebt.ac.cn (Y.Y.).

ORCID

Tao Song: 0000-0003-2088-8177
Yong Yang: 0000-0002-6118-5200

Notes

The authors declare no competing financial interest.

ACKNOWLEDGMENTS

The authors would like to acknowledge the financial support from DICP & QIBEBT (Grant No. DICP & QIBEBT UN201704), the Dalian National Laboratory for Clean Energy (DNL), Chinese Academy of Sciences, Key R Plan of Shandong Province (2019GGX102075), and Open Projects of State Key Laboratory of Physical Chemistry of the Solid Surface (Xiamen University) (No. 201808). Y.Y also acknowledges the support from the Royal Society (UK) for a Newton Advanced Fellowship (NAF\R2\180695).

REFERENCES

(1) Leeson, P. D.; Springthorpe, B. The influence of drug-like concepts on decision-making in medicinal chemistry. *Nat. Rev. Drug Discovery* **2007**, *6*, 881−890.
(2) Katritzky, A. R.; Rees, C. W.; Scriven, E. F. V.; *Comprehensive heterocyclic chemistry II*; Elsevier: Oxford. 1996.
(3) Bedi, P. M. S.; Kumar, V.; Mahajan, M. P. Synthesis and biological activity of novel antibacterial quinazolines. *Bioorg. Med. Chem. Lett.* **2004**, *14*, 5211−5213.
(4) Michael, J. P. Quinoline, quinazoline and acridone alkaloids. *Nat. Prod. Rep.* **2007**, *24*, 223−246.
(5) Horton, D. A.; Bourne, G. T.; Smythe, M. L. The combinatorial synthesis of bicyclic privileged structures or privileged substructures. *Chem. Rev.* **2003**, *103*, 893−930.
(6) Van Horn, K. S.; Burda, W. N.; Fleeman, R.; Shaw, L. N.; Manetsch, R. Antibacterial activity of a series of N^2, N^4-disubstituted quinazoline-2, 4-diamines. *J. Med. Chem.* **2014**, *57*, 3075−3093.
(7) Kung, P.-P.; Casper, M. D.; Cook, K. L.; Wilson Lingardo, L.; Risen, L. M.; Vickers, T. A.; Ranken, R.; Blyn, L. B.; Wyatt, J. R.; Cook, P. D.; Ecker, D. J. Structure-activity relationships of novel 2-substituted quinazoline antibacterial agents. *J. Med. Chem.* **1999**, *42*, 4705−4713.
(8) Khabnadideh, S.; Rezaei, Z.; Khalafi-Nezhad, A.; Bahrinajafi, R.; Mohamadi, R.; Farrokhroz, A. A. Synthesis of *N*-alkylated derivatives of imidazole as antibacterial agents. *Bioorg. Med. Chem. Lett.* **2003**, *13*, 2863−2865.
(9) Schleiss, M.; Eickhoff, J.; Auerochs, S.; Leis, M.; Abele, S.; Rechter, S.; Choi, Y.; Anderson, J.; Scott, G.; Rawlinson, W.; Michel, D.; Ensminger, S.; Klebl, B.; Stamminger, T.; Marschall, M. Protein

DOI: 10.1021/acssuschemeng.9b05298
ACS Sustainable Chem. Eng. 2020, 8, 267−277

kinase inhibitors of the quinazoline class exert anti-cytomegaloviral activity *in vitro* and *in vivo*. *Antiviral Res.* **2008**, *79*, 49−61.
(10) Párkányi, C.; Yuan, H. L.; Strömberg, B. H. E.; Evenzahav, A. Synthesis of 5-fluoro-2-methyl-3-(2-trifluoromethyl-1,3,4-thiadiazol-5-yl)-4(3H)-quinazolinone and related compounds with potential antiviral and anticancer activity. *J. Heterocycl. Chem.* **1992**, *29*, 749−753.
(11) Sharma, D.; Narasimhan, B.; Kumar, P.; Judge, V.; Narang, R.; de Clercq, E.; Balzarini, J. Synthesis, antimicrobial and antiviral evaluation of substituted imidazole derivatives. *Eur. J. Med. Chem.* **2009**, *44*, 2347−2353.
(12) Henderson, E. A.; Bavetsias, V.; Theti, D. S.; Wilson, S. C.; Clauss, R.; Jackman, A. L. Targeting the α-folate receptor with cyclopenta[g]quinazoline-based inhibitors of thymidylate synthase. *Bioorg. Med. Chem.* **2006**, *14*, 5020−5042.
(13) Marzaro, G.; Guiotto, A.; Chilin, A. Quinazoline derivatives as potential anticancer agents: a patent review (2007 − 2010). *Expert Opin. Ther Pat.* **2012**, *22*, 223−252.
(14) Baviskar, A. T.; Madaan, C.; Preet, R.; Mohapatra, P.; Jain, V.; Agarwal, A.; Guchhait, S. K.; Kundu, C. N.; Banerjee, U. C.; Bharatam, P. V. *N*-Fused imidazoles as novel anticancer agents that inhibit catalytic activity of topoisomerase IIα and induce apoptosis in G1/S phase. *J. Med. Chem.* **2011**, *54*, 5013−5030.
(15) Yamaguchi, F. T.; Sakairi, K.; Yamaguchi, E.; Tada, N.; Itoh, A. Magnesium iodide-catalyzed synthesis of 2-substituted quinazolines using molecular oxygen and visible light. *RSC Adv.* **2016**, *6*, 56892−56895.
(16) Ma, J.; Wan, Y.; Hong, C.; Li, M.; Hu, X.; Mo, W.; Hu, B.; Sun, N.; Jin, L.; Shen, Z. ABNO-catalyzed aerobic oxidative synthesis of 2-substituted 4H-3,1-benzoxazines and quinazolines. *Eur. J. Org. Chem.* **2017**, 3335−3342.
(17) Chen, X.; Chen, T.; Ji, F.; Zhou, Y.; Yin, S.-F. Iron-catalyzed aerobic oxidative functionalization of sp^3 C-H bonds: a versatile strategy for the construction of *N*-heterocycles. *Catal. Sci. Technol.* **2015**, *5*, 2197−2202.
(18) Zhang, Z.-H.; Zhang, X.-N.; Mo, L.-P.; Li, Y.-X.; Ma, F.-P. Catalyst-free synthesis of quinazoline derivatives using low melting sugar-urea-salt mixture as a solvent. *Green Chem.* **2012**, *14*, 1502−1506.
(19) Zhang, J.; Yu, C.; Wang, S.; Wan, C.; Wang, Z. A novel and efficient methodology for the construction of quinazolines based on supported copper oxide. *Chem. Commun.* **2010**, *46*, 5244−5246.
(20) Chatterjee, T.; Kim, D. I.; Cho, E. J. Base-promoted synthesis of 2-aryl quinazolines from 2-aminobenzylamines in water. *J. Org. Chem.* **2018**, *83*, 7423−7430.
(21) Yamaguchi, T.; Sugiura, Y.; Yamaguchi, E.; Tada, N.; Itoh, A. Synthetic method for the preparation of quinazolines by the oxidation of amines using singlet oxygen. *Asian J. Org. Chem.* **2017**, *6*, 432−435.
(22) Zhang, L.; Li, J.; Hu, Z.; Dong, J.; Zhang, X.-M.; Xu, X. Silver-catalyzed isocyanide insertion into N-H bond of ammonia: [5+1] annulation to quinazoline derivatives. *Adv. Synth. Catal.* **2018**, *360*, 1938−1942.
(23) Wang, H.; Chen, H.; Chen, Y.; Deng, G.-J. Palladium-catalyzed one pot 2-arylquinazoline formation via hydrogen-transfer strategy. *Org. Biomol. Chem.* **2014**, *12*, 7792−7799.
(24) Portela-Cubillo, F.; Scott, J. S.; Walton, J. C. 2-(Aminoaryl) alkanone O-phenyl oximes: versatile reagents for syntheses of quinazolines. *Chem. Commun.* **2008**, 2935−2937.
(25) Wang, C.; Li, S.; Liu, H.; Jiang, Y.; Fu, H. Copper-catalyzed synthesis of quinazoline derivatives via ullmann-type coupling and aerobic oxidation. *J. Org. Chem.* **2010**, *75*, 7936−7938.
(26) Malakar, C. C.; Baskakova, A.; Conrad, J.; Beifuss, U. Copper-catalyzed synthesis of quinazolines in water starting from *o*-bromobenzylbromides and benzamidines. *Chem. − Eur. J.* **2012**, *18*, 8882−8885.
(27) Lv, Y.; Li, Y.; Xiong, T.; Pu, W.; Zhang, H.; Sun, K.; Liu, Q.; Zhang, Q. Copper-catalyzed annulation of amidines for quinazoline synthesis. *Chem. Commun.* **2013**, *49*, 6439−6441.
(28) Cheng, X.; Wang, H.; Xiao, F.; Deng, G.-J. Lewis acid-catalyzed 2-arylquinazoline formation from *N*-arylbenzimidamides and paraformaldehyde. *Green Chem.* **2016**, *18*, 5773−5776.
(29) Lin, J.-P.; Zhang, F.-H.; Long, Y.-Q. Solvent/oxidant-switchable synthesis of multisubstituted quinazolines and benzimidazoles via metal-free selective oxidative annulation of arylamidines. *Org. Lett.* **2014**, *16*, 2822−2825.
(30) Wang, J.; Zha, S.; Chen, K.; Zhang, F.; Song, C.; Zhu, J. Quinazoline synthesis via Rh (III)-catalyzed intermolecular C-H functionalization of benzimidates with dioxazolones. *Org. Lett.* **2016**, *18*, 2062−2065.
(31) Han, B.; Wang, C.; Han, R.-F.; Yu, W.; Duan, X.-Y.; Fang, R.; Yang, X.-L. Efficient aerobic oxidative synthesis of 2-aryl quinazolines via benzyl C-H bond amination catalyzed by 4-hydroxy-TEMPO. *Chem. Commun.* **2011**, *47*, 7818−7820.
(32) Yao, S.; Zhou, K.; Wang, J.; Cao, H.; Yu, L.; Wu, J.; Qiu, P.; Xu, Q. Synthesis of 2-substituted quinazolines by CsOH-mediated direct aerobic oxidative cyclocondensation of 2-aminoarylmethanols with nitriles in air. *Green Chem.* **2017**, *19*, 2945−2951.
(33) Yan, Y.; Zhang, Y.; Feng, C.; Zha, Z.; Wang, Z. Selective iodine-catalyzed intermolecular oxidative amination of C(sp^3)-H bonds with *ortho*-carbonyl-substituted anilines to give quinazolines. *Angew. Chem., Int. Ed.* **2012**, *51*, 8077−8081.
(34) Chen, Z.; Chen, J.; Liu, M.; Ding, J.; Gao, W.; Huang, X.; Wu, H. Unexpected copper-catalyzed cascade synthesis of quinazoline derivatives. *J. Org. Chem.* **2013**, *78*, 11342−11348.
(35) Wang, Q.; Wang, F.; Yang, X.; Zhou, X.; Li, X. Rh(III)- and Zn(II)-catalyzed synthesis of quinazoline *N*-oxides via C-H amidation-cyclization of oximes. *Org. Lett.* **2016**, *18*, 6144−6147.
(36) He, L.; Li, H.; Chen, J.; Wu, X.-F. Recent advances in 4 (3 H)-quinazolinone syntheses. *RSC Adv.* **2014**, *4*, 12065−12077.
(37) Khan, I.; Ibrar, A.; Ahmed, W.; Saeed, A. Synthetic approaches, functionalization and therapeutic potential of quinazoline and quinazolinone skeletons: the advances continue. *Eur. J. Med. Chem.* **2015**, *90*, 124−169.
(38) Rohokale, R.; Kshirsagar, U. Advanced synthetic strategies for constructing quinazolinone scaffolds. *Synthesis* **2016**, *48*, 1253−1268.
(39) Maiden, T. M. M.; Harrity, J. P. A. Recent developments in transition metal catalysis for quinazolinone synthesis. *Org. Biomol. Chem.* **2016**, *14*, 8014−8025.
(40) Abdou, I. M.; Al-Neyadi, S. S. Synthesis of quinazolines and quinazolinones via palladium-mediated approach. *Heterocycl. Commun.* **2015**, *21*, 115−132.
(41) Abe, T.; Kida, K.; Yamada, K. A copper-catalyzed ritter-type cascade via iminoketene for the synthesis of quinazolin-4(3H)-ones and diazocines. *Chem. Commun.* **2017**, *53*, 4362−4365.
(42) Li, F.; Lu, L.; Ma, J. Acceptorless dehydrogenative condensation of *o*-aminobenzamides with aldehydes to quinazolinones in water catalyzed by a water-soluble iridium complex [Cp*Ir(H_2O)$_3$][OTf]$_2$. *Org. Chem. Front.* **2015**, *2*, 1589−1597.
(43) Parashuram, L.; Sreenivasa, S.; Akshatha, S.; Kumar, V. U.; Kumar, S. Zirconia-supported Cu(I)-stabilized copper oxide mesoporous catalyst for the synthesis of quinazolinones under ambient conditions. *Asian J. Org. Chem.* **2017**, *6*, 1755−1759.
(44) Chen, X.; Chen, T.; Ji, F.; Zhou, Y.; Yin, S.-F. Iron-catalyzed aerobic oxidative functionalization of sp3C-H bonds: a versatile strategy for the construction of *N*-heterocycles. *Catal. Sci. Technol.* **2015**, *5*, 2197−2202.
(45) Zhu, Y.-P.; Fei, Z.; Liu, M.-C.; Jia, F.-C.; Wu, A.-X. Direct one-pot synthesis of luotonin F and analogues via rational logical design. *Org. Lett.* **2013**, *15*, 378−381.
(46) Li, Q.; Huang, Y.; Chen, T.; Zhou, Y.; Xu, Q.; Yin, S.-F.; Han, L.-B. Copper-catalyzed aerobic oxidative amination of sp^3C-H bonds: efficient synthesis of 2-hetarylquinazolin-4(3H)-ones. *Org. Lett.* **2014**, *16*, 3672−3675.
(47) Xu, G.; Wang, L.; Li, M.; Tao, M.; Zhang, W. Phosphorous acid functionalized polyacrylonitrile fibers with a polarity tunable surface micro-environment for one-pot C-C and C-N bond formation reactions. *Green Chem.* **2017**, *19*, 5818−5830.

DOI: 10.1021/acssuschemeng.9b05298
ACS Sustainable Chem. Eng. 2020, 8, 267−277

(48) Laha, J. K.; Patel, K. V.; Tummalapalli, K. S. S.; Dayal, N. Formation of amides, their intramolecular reactions for the synthesis of *N*-heterocycles, and preparation of a marketed drug, sildenafil: a comprehensive coverage. *Chem. Commun.* **2016**, *52*, 10245−10248.
(49) Zhao, D.; Wang, T.; Li, J.-X. Metal-free oxidative synthesis of quinazolinones via dual amination of sp^3C-H bonds. *Chem. Commun.* **2014**, *50*, 6471−6474.
(50) Li, Z.; Dong, J.; Chen, X.; Li, Q.; Zhou, Y.; Yin, S.-F. Metal- and oxidant-free synthesis of quinazolinones from *β*-ketoesters with *o*-aminobenzamides via phosphorous acid-catalyzed cyclocondensation and selective C-C Bond Cleavage. *J. Org. Chem.* **2015**, *80*, 9392−9400.
(51) Chen, X.; Chen, T.; Zhou, Y.; Han, D.; Han, L.-B.; Yin, S.-F. Metal-free aerobic oxidative C-N bond cleavage of tertiary amines for the synthesis of *N*-heterocycles with high atom efficiency. *Org. Biomol. Chem.* **2014**, *12*, 3802−3807.
(52) Modi, A.; Ali, W.; Mohanta, P. R.; Khatun, N.; Patel, B. K. CuO nanoparticle catalyzed synthesis of 2,3-disubstituted quinazolinones via sequential *N*-arylation and oxidative C-H amidation. *ACS Sustainable Chem. Eng.* **2015**, *3*, 2582−2590.
(53) Battula, S.; Vishwakarma, R. A.; Ahmed, Q. N. Cu-benzotriazole-catalyzed electrophilic cyclization of *N*-arylimines: a methodical tandem approach to O-protected-4-hydroxyquinazolines. *RSC Adv.* **2014**, *4*, 38375−38378.
(54) Jiang, X.; Tang, T.; Wang, J.-M.; Chen, Z.; Zhu, Y.-M.; Ji, S.-J. Palladium-catalyzed one-pot synthesis of quinazolinones via tert-butyl isocyanide insertion. *J. Org. Chem.* **2014**, *79*, 5082−5087.
(55) Li, H.; He, L.; Neumann, H.; Beller, M.; Wu, X.-F. Cascade synthesis of quinazolinones from 2-aminobenzonitriles and aryl bromides via palladium-catalyzed carbonylation reaction. *Green Chem.* **2014**, *16*, 1336−1343.
(56) Wu, X.-F.; He, L.; Neumann, H.; Beller, M. Palladium-catalyzed carbonylative synthesis of quinazolinones from 2-aminobenzamide and aryl bromides. *Chem. − Eur. J.* **2013**, *19*, 12635−12638.
(57) Upadhyaya, K.; Thakur, R. K.; Shukla, S. K.; Tripathi, R. P. One-pot copper (I)-catalyzed ligand/base-free tandem cyclooxidative synthesis of quinazolinones. *J. Org. Chem.* **2016**, *81*, 5046−5055.
(58) Yu, X.; Gao, L.; Jia, L.; Yamamoto, Y.; Bao, M. Synthesis of quinazolin-4(3H)-ones via the reaction of 2-halobenzamides with nitriles. *J. Org. Chem.* **2018**, *83*, 10352−10358.
(59) Jia, F.-C.; Zhou, Z.-W.; Xu, C.; Cai, Q.; Li, D.-K.; Wu, A.-X. Expeditious synthesis of 2-phenylquinazolin-4-amines via a Fe/Cu relay-catalyzed domino strategy. *Org. Lett.* **2015**, *17*, 4236−4239.
(60) Kasprzak, A.; Bystrzejewski, M.; Poplawska, M. Sulfonated carbon-encapsulated iron nanoparticles as an efficient magnetic nanocatalyst for highly selective synthesis of benzimidazoles. *Dalton Trans.* **2018**, *47*, 6314−6322.
(61) Kawashita, Y.; Nakamichi, N.; Kawabata, H.; Hayashi, M. Direct and practical synthesis of 2-arylbenzoxazoles promoted by activated carbon. *Org. Lett.* **2003**, *5*, 3713−3715.
(62) Trivedi, R.; De, S. K.; Gibbs, R. A. A convenient one-pot synthesis of 2-substituted benzimidazoles. *J. Mol. Catal. A: Chem.* **2006**, *245*, 8−11.
(63) Bahrami, K.; Khodaei, M. M.; Naali, F. Mild and highly efficient method for the synthesis of 2-arylbenzimidazoles and 2-arylbenzothiazoles. *J. Org. Chem.* **2008**, *73*, 6835−6837.
(64) Chen, Y. X.; Qian, L.-F.; Zhang, W.; Han, B. Efficient aerobic oxidative synthesis of 2-substituted benzoxazoles, benzothiazoles, and benzimidazoles catalyzed by 4-methoxy-TEMPO. *Angew. Chem., Int. Ed.* **2008**, *47*, 9330−9333.
(65) Zhang, C.; Zhang, L.; Jiao, N. Catalyst free approach to benzimidazoles using air as the oxidant at room temperature. *Green Chem.* **2012**, *14*, 3273−3276.
(66) Grimmet, M. R.; Katritzky, A. R.; Rees, C. W. *Comprehensive heterocyclic chemistry*; Elsevier, 1984, Vol. *5*, p 457.
(67) Middleton, R. W.; Wibberley, D. G. Synthesis of imidazo[4,5-b]-and[4,5-c]-pyridines. *J. Heterocycl. Chem.* **1980**, *17*, 1757−1760.
(68) Czarny, A.; Wilson, W. D.; Boykin, D. W. Synthesis of monocationic and dicationic analogs of hoechst 33258. *J. Heterocycl. Chem.* **1996**, *33*, 1393−1397.
(69) Brasche, G.; Buchwald, S. L. C-H functionalization/C-N bond formation: copper-catalyzed synthesis of benzimidazoles from amidines. *Angew. Chem., Int. Ed.* **2008**, *47*, 1932−1934.
(70) Brain, C. T.; Steer, J. T. An improved procedure for the synthesis of benzimidazoles, using palladium-catalyzed aryl-amination chemistry. *J. Org. Chem.* **2003**, *68*, 6814−6816.
(71) Peng, J.; Ye, M.; Zong, C.; Hu, F.; Feng, L.; Wang, X.; Wang, Y.; Chen, C. Copper-catalyzed intramolecular C-N bond formation: A straightforward synthesis of benzimidazole derivatives in water. *J. Org. Chem.* **2011**, *76*, 716−719.
(72) Li, C. J.; Li, Z. Green chemistry: the development of cross-dehydrogenative coupling (CDC) for chemical synthesis. *Pure Appl. Chem.* **2006**, *78*, 935−945.
(73) Yoo, W. J.; Li, C. J. *Cross-dehydrogenative coupling reactions of sp3-hybridized C-H bonds, C-H activation*; Springer: Berlin, Heidelberg, 2009: 281−302.
(74) Li, C. J. Cross-dehydrogenative coupling (CDC): exploring C-C bond formations beyond functional group transformations. *Acc. Chem. Res.* **2009**, *42*, 335−344.
(75) Hakim Siddiki, S. M. A.; Kon, K.; Touchy, A. S.; Shimizu, K.-I. Direct synthesis of quinazolinones by acceptorless dehydrogenative coupling of o-aminobenzamide and alcohols by heterogeneous Pt catalysts. *Catal. Sci. Technol.* **2014**, *4*, 1716−1719.
(76) Shiraishi, Y.; Sugano, Y.; Tanaka, S.; Hirai, T. One-pot synthesis of benzimidazoles by simultaneous photocatalytic and catalytic reactions on Pt@TiO_2 nanoparticles. *Angew. Chem., Int. Ed.* **2010**, *49*, 1656−1660.
(77) Hikawa, H.; Ino, Y.; Suzuki, H.; Yokoyama, Y. Pd-catalyzed benzylic C-H amidation with benzyl alcohols in water: a strategy to construct quinazolinones. *J. Org. Chem.* **2012**, *77*, 7046−7051.
(78) Guan, Q.; Sun, Q.; Wen, L.; Zha, Z.; Yang, Y.; Wang, Z. The synthesis of benzimidazoles via a recycled palladium catalysed hydrogen transfer under mild conditions. *Org. Biomol. Chem.* **2018**, *16*, 2088−2096.
(79) Feng, F.; Ye, J.; Cheng, Z.; Xu, X.; Zhang, Q.; Ma, L.; Lu, C.; Li, X. Cu-Pd/γ-Al_2O_3 catalyzed the coupling of multi-step reactions: direct synthesis of benzimidazole derivatives. *RSC Adv.* **2016**, *6*, 72750−72755.
(80) Zhou, J.; Fang, J. One-pot synthesis of quinazolinones via iridium-catalyzed hydrogen transfers. *J. Org. Chem.* **2011**, *76*, 7730−7736.
(81) Li, F.; Lu, L.; Liu, P. Acceptorless dehydrogenative coupling of *o*-aminobenzamides with the activation of methanol as a C1 source for the construction of quinazolinones. *Org. Lett.* **2016**, *18*, 2580−2583.
(82) Takeyama, K.; Wada, K.; Miura, H.; Hosokawa, S.; Abe, R.; Inoue, M. Dehydrogenative synthesis of benzimidazoles under mild conditions with supported iridium catalysts. *Catal. Sci. Technol.* **2016**, *6*, 1677−1684.
(83) Watson, A. J. A.; Maxwell, A. C.; Williams, J. M. J. Ruthenium-catalysed oxidative synthesis of heterocycles from alcohols. *Org. Biomol. Chem.* **2012**, *10*, 240−243.
(84) Zhang, W.; Meng, C.; Liu, Y.; Tang, Y.; Li, F. Auto-tandem catalysis with ruthenium: from *o*-aminobenzamides and allylic alcohols to quinazolinones via redox isomerization/acceptorless dehydrogenation. *Adv. Synth. Catal.* **2018**, *360*, 3751−3759.
(85) Li, L.; Luo, Q.; Cui, H.; Li, R.; Zhang, J.; Peng, T. Air-stable ruthenium(II)-NNN pincer complexes for the efficient coupling of aromatic diamines and alcohols to 1H-benzo[d]imidazoles with the Liberation of H_2. *ChemCatChem* **2018**, *10*, 1607.
(86) Tang, L.; Yang, Y.; Wen, L.; Zhang, S.; Zha, Z.; Wang, Z. Supported gold-catalyzed and ammonia-promoted selective synthesis of quinazolines in aqueous media. *Org. Chem. Front.* **2015**, *2*, 114−118.
(87) Tang, L.; Zhao, X.; Zou, G.; Zhou, Y.; Yang, X. Heterogeneous gold-catalyzed cascade hydrogen-transfer strategy for selective syn-

DOI: 10.1021/acssuschemeng.9b05298
ACS Sustainable Chem. Eng. 2020, 8, 267−277

thesis of quinazolinones in water. *Asian J. Org. Chem.* **2016**, *5*, 335−339.
(88) Tang, L.; Guo, X.; Yang, Y.; Zha, Z.; Wang, Z. Gold nanoparticles supported on titanium dioxide: an efficient catalyst for highly selective synthesis of benzoxazoles and benzimidazoles. *Chem. Commun.* **2014**, *50*, 6145−6148.
(89) Daw, P.; Ben-David, Y.; Milstein, D. Direct synthesis of benzimidazoles by dehydrogenative coupling of aromatic diamines and alcohols catalyzed by cobalt. *ACS Catal.* **2017**, *7*, 7456−7460.
(90) Xu, Z.; Yu, X.; Sang, X.; Wang, D. BINAP-copper supported by hydrotalcite as an efficient catalyst for the borrowing hydrogen reaction and dehydrogenation cyclization under water or solvent-free conditions. *Green Chem.* **2018**, *20*, 2571−2577.
(91) Xu, Z.; Wang, D.-S.; Yu, X.; Yang, Y.; Wang, D. Tunable triazole-phosphine-copper catalysts for the Synthesis of 2-aryl-1H-benzo[d]imidazoles from benzyl alcohols and diamines by acceptorless dehydrogenation and borrowing hydrogen reactions. *Adv. Synth. Catal.* **2017**, *359*, 3332−3340.
(92) Parua, S.; Sikari, R.; Sinha, S.; Chakraborty, G.; Mondal, R.; Paul, N. D. Accessing polysubstituted quinazolines via nickel catalyzed acceptorless dehydrogenative coupling. *J. Org. Chem.* **2018**, *83*, 11154−11166.
(93) Bera, A.; Sk, M.; Singh, K.; Banerjee, D. Nickel-catalysed dehydrogenative coupling of aromatic diamines with alcohols: selective synthesis of substituted benzimidazoles and quinoxalines. *Chem. Commun.* **2019**, *55*, 5958−5961.
(94) Chakraborty, G.; Sikari, R.; Das, S.; Mondal, R.; Sinha, S.; Banerjee, S.; Paul, N. D. Dehydrogenative synthesis of quinolines, 2-aminoquinolines and quinazolines using singlet di-radical Ni (II)-catalysts. *J. Org. Chem.* **2019**, *84*, 2626−2641.
(95) Das, K.; Mondal, A.; Srimani, D. Selective synthesis of 2-substituted and 1,2-disubstituted benzimidazoles directly from aromatic diamines and alcohols catalyzed by molecularly defined nonphosphine manganese (I) complex. *J. Org. Chem.* **2018**, *83*, 9553−9560.
(96) Zhao, D.; Zhou, Y.-R.; Shen, Q.; Li, J.-X. Iron-catalyzed oxidative synthesis of *N*-heterocycles from primary alcohols. *RSC Adv.* **2014**, *4*, 6486−6489.
(97) Oveisi, A. R.; Khorramabadi-zad, A.; Daliran, S. Iron-based metal-organic framework, Fe(BTC): an effective dual-functional catalyst for oxidative cyclization of bisnaphthols and tandem synthesis of quinazolin-4(3H)-ones. *RSC Adv.* **2016**, *6*, 1136−1142.
(98) Zhang, Z.; Wang, M.; Zhang, C.; Zhang, Z.; Lu, J.; Wang, F. The cascade synthesis of quinazolinones and quinazolines using an α-MnO_2 catalyst and tert-butyl hydroperoxide (TBHP) as an oxidant. *Chem. Commun.* **2015**, *51*, 9205−9207.
(99) Ju, J.; Hua, R.; Su, J. Copper-catalyzed three-component one-pot synthesis of quinazolines. *Tetrahedron* **2012**, *68*, 9364−9370.
(100) Wang, Y.; Meng, X.; Chen, G.; Zhao, P. Direct synthesis of quinazolinones by heterogeneous Cu $(OH)_x$/OMS-2 catalyst under oxygen. *Catal. Commun.* **2018**, *104*, 106−111.
(101) Mahesh, D.; Sadhu, P.; Punniyamurthy, T. Copper (II)-catalyzed oxidative cross-coupling of anilines, primary alkyl amines, and sodium azide using TBHP: a route to 2-substituted benzimidazoles. *J. Org. Chem.* **2016**, *81*, 3227.
(102) Eskandari, A.; Jafarpour, M.; Rezaeifard, A.; Salimi, M. A dendritic TiO_2-Co (II) nanocomposite based on the melamine catalyzed one-pot aerobic photocatalytic synthesis of benzimidazoles. *New J. Chem.* **2018**, *42*, 6449−6456.
(103) Reddy, P. L.; Arundhathi, R.; Tripathi, M.; Chauhan, P.; Yan, N.; Rawat, D. S. Solvent-free oxidative synthesis of 2-substituted benzimidazoles by immobilized cobalt oxide nanoparticles on alumina/silica support. *ChemistrySelect* **2017**, *2*, 3889−3895.
(104) Wu, W.; Jiang, H. Palladium-catalyzed oxidation of unsaturated hydrocarbons using molecular oxygen. *Acc. Chem. Res.* **2012**, *45*, 1736−1748.
(105) Tang, X.; Wu, W.; Zeng, W.; Jiang, H. Copper-catalyzed oxidative carbon-carbon and/or carbon−heteroatom bond formation with O_2 or internal oxidants. *Acc. Chem. Res.* **2018**, *51*, 1092−1105.
(106) Liang, Y.-F.; Jiao, N. Oxygenation via C-H/C-C bond activation with molecular oxygen. *Acc. Chem. Res.* **2017**, *50*, 1640−1653.
(107) Li, X.; Rao, J.; Ouyang, W.; Chen, Q.; Cai, N.; Lu, Y.-J.; Huo, Y. Sequential C-H and C-C bond cleavage: divergent constructions of fused *N*-heterocycles via tunable cascade. *ACS Catal.* **2019**, *9*, 8749−8756.
(108) Li, X.; Huang, L.; Chen, J.; Wu, W.; Huang, H.; Jiang, H. Copper-catalyzed oxidative [2+2+1] cycloaddition: regioselective synthesis of 1, 3-oxazoles from internal alkynes and nitriles. *Chem. Sci.* **2012**, *3*, 3463−3467.
(109) Li, X.; He, L.; Chen, H.; Wu, W.; Jiang, H. Copper-catalyzed aerobic C(sp^2)-H functionalization for C-N bond formation: synthesis of pyrazoles and indazoles. *J. Org. Chem.* **2013**, *78*, 3636−3646.
(110) Song, T.; Ren, P.; Duan, Y.; Wang, Z.; Chen, X.; Yang, Y. Cobalt nanocomposites on N-doped hierarchical porous carbon for highly selective formation of anilines and imines from nitroarenes. *Green Chem.* **2018**, *20*, 4629−4637.
(111) Song, T.; Ma, Z.; Yang, Y. Chemoselective hydrogenation of α, β-unsaturated carbonyls catalyzed by biomass-derived cobalt nanoparticles in Water. *ChemCatChem* **2019**, *11*, 1313−1319.
(112) Duan, Y.; Song, T.; Dong, X.; Yang, Y. Enhanced catalytic performance of cobalt nanoparticles coated with a N, P-codoped carbon shell derived from biomass for transfer hydrogenation of functionalized nitroarenes. *Green Chem.* **2018**, *20*, 2821−2828.
(113) Dong, X.; Wang, Z.; Duan, Y.; Yang, Y. One-pot selective *N*-formylation of nitroarenes to formamides catalyzed by core-shell structured cobalt nanoparticles. *Chem. Commun.* **2018**, *54*, 8913−8916.
(114) Duan, Y.; Ji, G.; Zhang, S.; Chen, X.; Yang, Y. Additive-modulated switchable reaction pathway in the addition of alkynes with organosilanes catalyzed by supported Pd nanoparticles: hydrosilylation versus semihydrogenation. *Catal. Sci. Technol.* **2018**, *8*, 1039−1050.
(115) Stern, L.-A.; Feng, L.; Song, F.; Hu, X. Ni_2P as a Janus catalyst for water splitting: the oxygen evolution activity of Ni_2P nanoparticles. *Energy Environ. Sci.* **2015**, *8*, 2347−2351.
(116) Xu, Y.; Sang, H.; Wang, K.; Wang, X. Catalytic dehydrogenation of isobutane in the presence of hydrogen over Cs-modified Ni_2P supported on active carbon. *Appl. Surf. Sci.* **2014**, *316*, 163−170.
(117) Miao, X.; Yin, R.; Ge, X.; Li, Z.; Yin, L. Ni_2P@carbon core-shell nanoparticle-arched 3D interconnected graphene aerogel architectures as anodes for high-performance sodium-ion batteries. *Small* **2017**, *13*, 1702138.
(118) Pan, Y.; Yang, N.; Chen, Y.; Lin, Y.; Li, Y.; Liu, Y.; Liu, C. Nickel phosphide nanoparticles-nitrogen-doped graphene hybrid as an efficient catalyst for enhanced hydrogen evolution activity. *J. Power Sources* **2015**, *297*, 45−52.
(119) Gordon, S. G.; Miller, M. W.; Saunders, A. B. Pimobendan in heart failure therapy -a silver bullet? *J. Am. Anim. Hosp. Assoc.* **2006**, *42*, 90−93.
(120) Das, J.; Singh, K.; Vellakkaran, M.; Banerjee, D. Nickel-Catalyzed Hydrogen-Borrowing Strategy for α-Alkylation of Ketones with Alcohols: A New Route to Branched gem-Bis(alkyl) Ketones. *Org. Lett.* **2018**, *20*, 5587−5591.
(121) Shimizu, K.-i.; Imaiida, N.; Kon, K.; Hakim Siddiki, S. M. A.; Satsuma, A. Heterogeneous Ni catalysts for *N*-alkylation of amines with alcohols. *ACS Catal.* **2013**, *3*, 998−1005.
(122) Su, H.; Gao, P.; Wang, M.-Y.; Zhai, G.-Y.; Zhang, J.-J.; Zhao, T.-J.; Su, J.; Antonietti, M.; Li, X.-H.; Chen, J.-S. Grouping Effect of Single Nickel−N_4 Sites in Nitrogen−Doped Carbon Boosts Hydrogen Transfer Coupling of Alcohols and Amines. *Angew. Chem., Int. Ed.* **2018**, *57*, 15194−15198.

DOI: 10.1021/acssuschemeng.9b05298
ACS Sustainable Chem. Eng. 2020, 8, 267−277